Electronic Supplementary Information

Origin of surface trap states in CdS quantum dots: Relationship between size dependent photoluminescence and sulfur vacancy trap states

Aisea Veamatahau,[a] Bo Jiang,[a] Tom Seifert,[a]† Satoshi Makuta,[a] Kay Latham,[b] Masayuki Kanehara,[c] Toshiharu Teranishi,[d] and Yasuhiro Tachibana*[a e f]

[a]School of Aerospace, Mechanical and Manufacturing Engineering, RMIT University, Bundoora, VIC 3083, Australia; [b]School of Applied Sciences, RMIT University, Melbourne, VIC 3001, Australia; [c]Research Core for Interdisciplinary Sciences, Okayama University, 3-1-1 Tsushimanaka, Okayama, Okayama 700-8530, Japan; [d]Institute for Chemical Research, Kyoto University, Gokasho, Uji, Kyoto 611-0011 (Japan); [e]Office for University-Industry Collaboration, Osaka University, 2-1 Yamada-oka, Suita, Osaka 565-0871, Japan; [f]Japan Science and Technology Agency (JST), PRESTO, 4-1-8 Honcho Kawaguchi, Saitama 332-0012, Japan

†Current address: PC Department, Fritz-Haber-Institut der Max-Planck-Gesellschaft, Faradayweg 4-6, 14195 Berlin, Germany.

EXPERIMENTAL

Synthesis of CdS QDs employing a different precursor, ligand and/or solvent

(i) Cadmium stearate (0.3 mmol), oleylamine (3.0 mmol) and 1,3-dibutyl-2-thiourea (0.15 mmol) were dispersed in 9 mL of diphenyl ether (Cd:S = 2:1). (ii) Cadmium stearate (0.3 mmol), octadecylamine (3.0 mmol) and 1,3-dibutyl-2-thiourea (0.15 mmol) were dispersed in 9 mL of diphenyl ether (Cd:S = 2:1). (iii) Cadmium stearate (0.3 mmol), oleylamine (3.0 mmol) and sulfur (0.15 mmol) were dispersed in 9 mL of di-n-octyl ether (Cd:S = 2:1). Oxygen and water were removed from the solution under vacuum at room temperature, and subsequently the solution was heated to 90~210 ºC under nitrogen atmosphere, forming CdS QDs. QD sizes of <3.2 nm were obtained by adjusting the heating temperature between 90 and 210 ºC, and the heating time. QD sizes greater than 3.2 nm were prepared simply by adding the same amount of precursors into the synthesized QD solution without purification, and by conducting the reaction at 210~250 ºC. After the final reaction, the synthesized QDs were purified with methanol, and subsequently acetone, and finally the QDs were dissolved in chloroform.

Transmission electron microscopy measurements

Electron microscopy images of the synthesized QDs were obtained by Hitachi H-9000NAR transmission electron microscopy (TEM) operated at 300 kV at the Research Center for Ultra-High Voltage Electron Microscopy in Osaka University. The samples were prepared by casting a drop of diluted QD solutions onto a 300-copper mesh grid coated by a carbon film, followed by drying them in air at room temperature.

Sensitivity calibration for XPS elemental analysis

The number of detected electrons (the intensity of XPS signal) has to be corrected for an atomic sensitivity factor, S, to determine composition (Cd/S ratio) of a quantum dot. Following

the previous reports,[1-3] Cd/S correction factors are calculated. In a homogeneous material, the intensity of a peak in XPS from a single element, I, is:

$$I = nf\sigma\theta y\Delta AT$$

where n is the number of atoms per cm^3, f is the X-ray flux, σ is the cross section for photoelectric processes, θ is an angular factor, y is the efficiency for formation of a photoelectron with the full kinetic energy, Δ is the mean escape depth of photoelectrons of that kinetic energy, A is the area probed and T is a factor for the efficiency of detecting electrons of a given kinetic energy. If the effects of elastic-electron scattering in a material are neglected and we consider only the direction of the XPS detector, the mean escape depth, Δ, becomes equivalent to the inelastic mean free path of the electrons, λ.[4] The number of atoms per cm^3 can then be determined:

$$n = \frac{I}{f\sigma\theta y\Delta AT} = \frac{I}{S}$$

where S is an atomic sensitivity factor, and would usually be provided in the instrument software. Relative concentrations of atoms in a thick flat material can be determined by dividing each peak intensity by its sensitivity factor and by taking the ratio. For QDs samples, this calibration requires further correction to account for the spherical particle geometry and the small QD size. This correction, (Cd/S)$_{corrected}$, is provided following the previous reports.[2, 3]

$$(Cd/S)_{corrected} = \frac{\lambda_{Cd}}{\int_0^d \exp\left[-\left(z/\lambda_{Cd}\right)\right]dz}\frac{\int_0^d \exp\left[-\left(z/\lambda_S\right)\right]dz}{\lambda_S}(Cd/S)$$

where d is the depth of material, and z is the distance from an arbitrary point within the QD to the surface in the direction of the detector.[1-3] To calculate the integral part in this equation, we introduce polar co-ordinates as shown in Fig. S1.
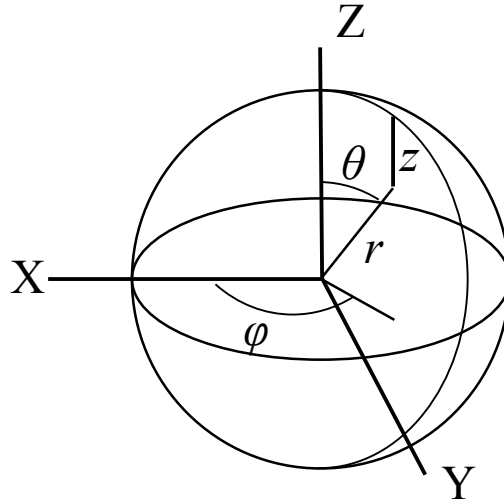
Fig. S1. Polar co-ordinates to describe the distance, z, from an arbitrary point within the spherical QD to the surface in the direction of the detector (Z axis).

$$\int_0^d \exp\left[-\left(z/\lambda\right)\right]dz = \int_0^{2\pi}\int_0^{\pi}\int_0^R r^2 \exp\left[-\frac{\sqrt{R^2 - r^2\sin^2\theta} - r\cos\theta}{\lambda}\right]dr\ \sin\theta\ d\theta\ d\varphi$$

where r is the distance from an arbitrary point within the spherical QD to the centre of the co-ordinate, θ is the angle between r and Z axis, φ is the angle between the horizontal component of

r and X axis, R is the radius of the QD. The inelastic mean free paths were estimated according to the method described in the previous report,[4] using the following equation:

$$\lambda = \frac{E}{E_p^2\left[\beta \ln(\gamma E) - \left(C/E\right) + \left(D/E^2\right)\right]}$$

$$\beta = -0.10 + 0.944\left(E_p^2 + E_g^2\right)^{-1/2} + 0.069\rho^{0.1}$$

$$\gamma = 0.191\rho^{-0.50}$$

$$C = 1.97 - 0.91\,U$$

$$D = 53.4 - 20.8\,U$$

$$U = \frac{N_V\rho}{M} = \frac{E_p^2}{829.4}$$

where E is the electron energy (in eV), E_p is the free electron plasmon energy (in eV), ρ is the density (in g/cm³), N_V is the number of valence electrons per molecule (for compounds), E_g is the band gap energy (in eV), and M is the molecular weight. For CdS, the molecular weight is 144.47 g/mol, the density is 4.82 g/cm³, the number of valence electrons is assumed to be 18, and the band gap of each QD size is taken as the first exciton peak shown in Table 1 in the main text. The calculated inelastic mean free paths for Cd 3d core and S 2p core for Al K_α radiation are summarized in Table S1. The correction factors were determined to be 0.911, 0.914, 0.919 and 0.927 for CdS QD with a diameter of 3.1, 3.3, 3.7 and 4.3 nm, respectively.

Table S1. Calculated inelastic mean free paths and correction factors.

| QD diameter / nm	λ_{Cd} / Å	λ_S / Å	(Cd/S) *corrected*
3.1	21.29	24.91	0.911
3.3	21.26	24.87	0.914
3.7	21.23	24.84	0.919
4.3	21.20	24.81	0.927

RESULTS

CdS QDs synthesized by employing a different precursor, ligand and/or solvent. Non-injection synthesis of CdS QDs was also performed using a different sulfur precursor, ligand and/or solvent. Here three cases, i.e. (i) diphenyl ether instead of di-n-octyl ether, (ii) octadecylamine and diphenyl ether instead of oleylamine and di-n-octyl ether, and (iii) sulfur instead of 1,3-dibutyl-2-thiourea, were employed to observe their influence on CdS QD exciton peak position and size distribution. Absorption spectra of CdS QDs obtained by employing (i) cadmium stearate (0.3 mmol), oleylamine (3.0 mmol) and 1,3-dibutyl-2-thiourea (0.15 mmol) dispersed in 9 mL of diphenyl ether (Cd:S = 2:1), (ii) cadmium stearate (0.3 mmol), octadecylamine (3.0 mmol) and 1,3-dibutyl-2-thiourea (0.15 mmol) dispersed in 9 mL of diphenyl ether (Cd:S = 2:1) and (iii) cadmium stearate (0.3 mmol), oleylamine (3.0 mmol) and sulfur (0.15 mmol) dispersed in 9 mL of di-n-octyl ether (Cd:S = 2:1) are shown in Fig. S2. All of the first exciton peaks are not distinctive compared to those obtained by employing cadmium stearate (0.3 mmol), oleylamine (3.0 mmol) and 1,3-dibutyl-2-thiourea (0.15 mmol) dispersed in 9 mL of di-n-octyl ether (Cd:S = 2:1).
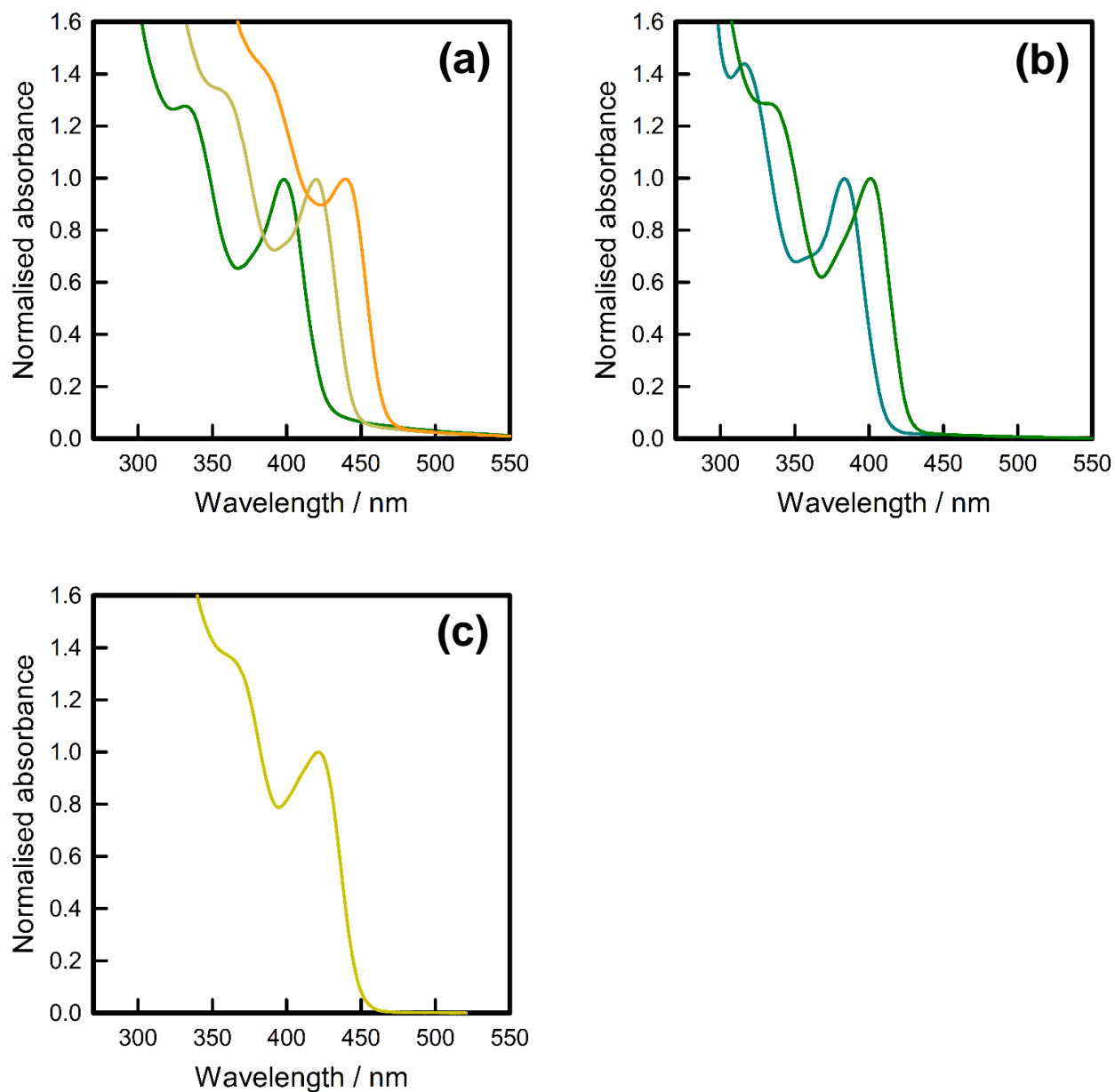
Fig. S2. Absorption spectra of CdS QDs obtained by employing (a) diphenyl ether instead of di-n-octyl ether, (b) octadecylamine and diphenyl ether instead of oleylamine and di-n-octyl ether, and (c) sulfur instead of 1,3-dibutyl-2-thiourea.

TEM measurements. TEM measurements were also conducted for CdS QDs with different sizes. Fig. S3 a, c, e and g show typical TEM images collected for CdS QDs with an average

diameter of 3.1, 3.3, 3.7 and 4.3 nm. The size histograms of these CdS QDs are shown in Fig. S3 b, d, f and h.
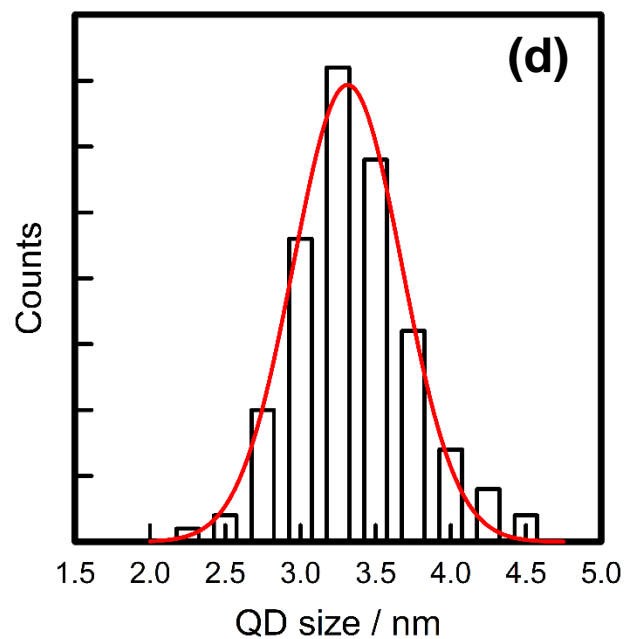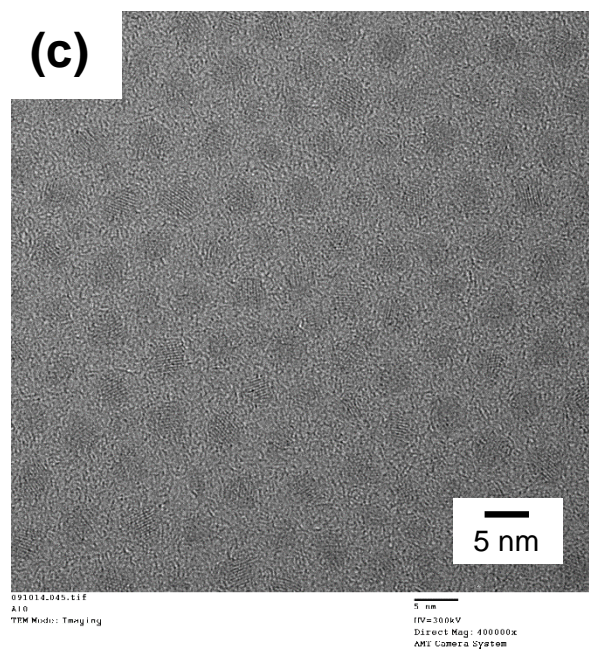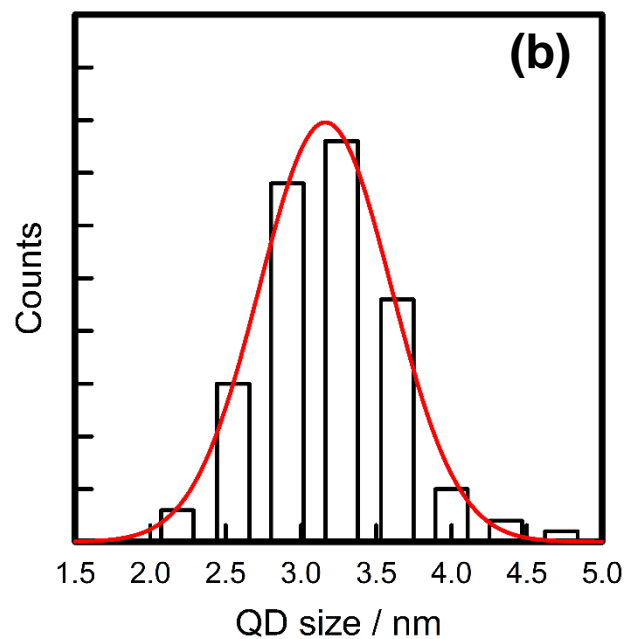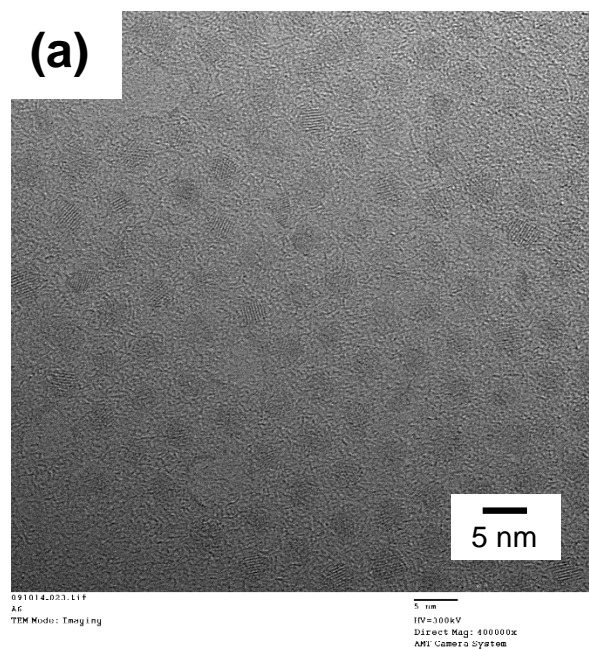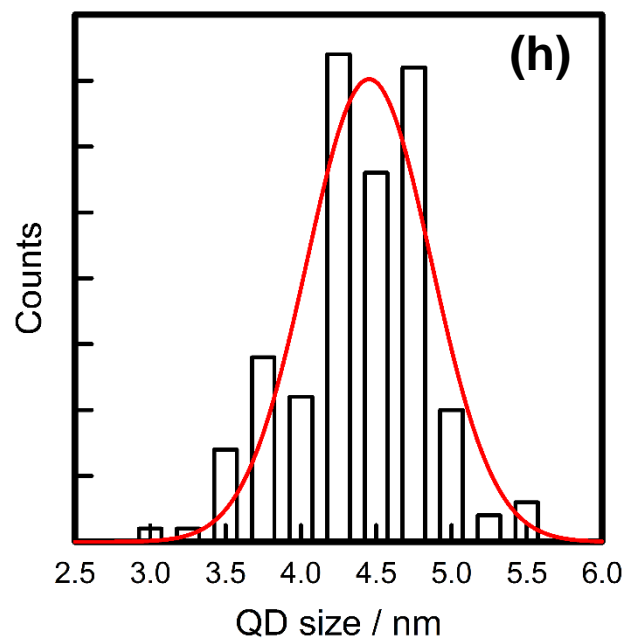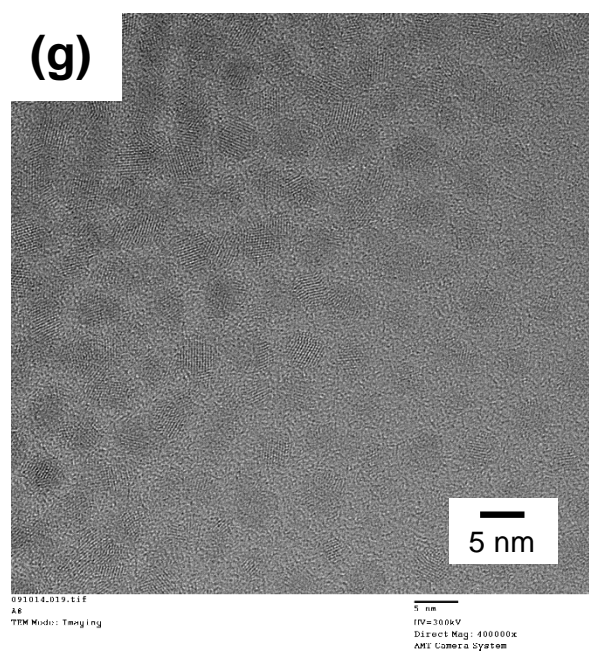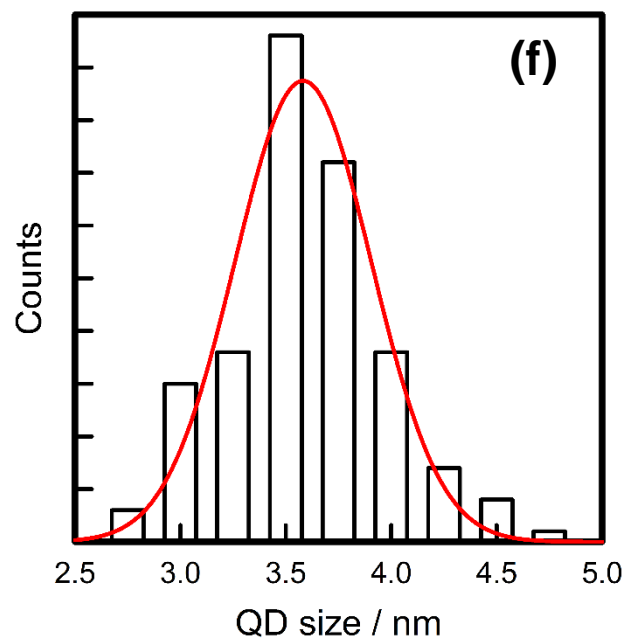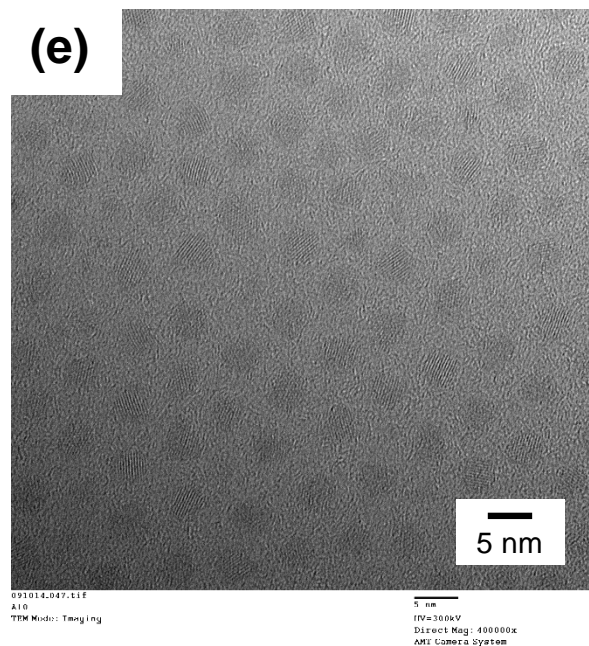
Fig. S3. TEM image of CdS QDs with an average diameter of (a) 3.1 nm, (c) 3.3 nm, (e) 3.7 nm and (g) 4.3 nm. A histogram of QD size with an average diameter of (b) 3.1 nm, (d) 3.3 nm, (f) 3.7 nm and (h) 4.3 nm. The red solid line shows Gaussian fitting with a distribution of around 10 %.
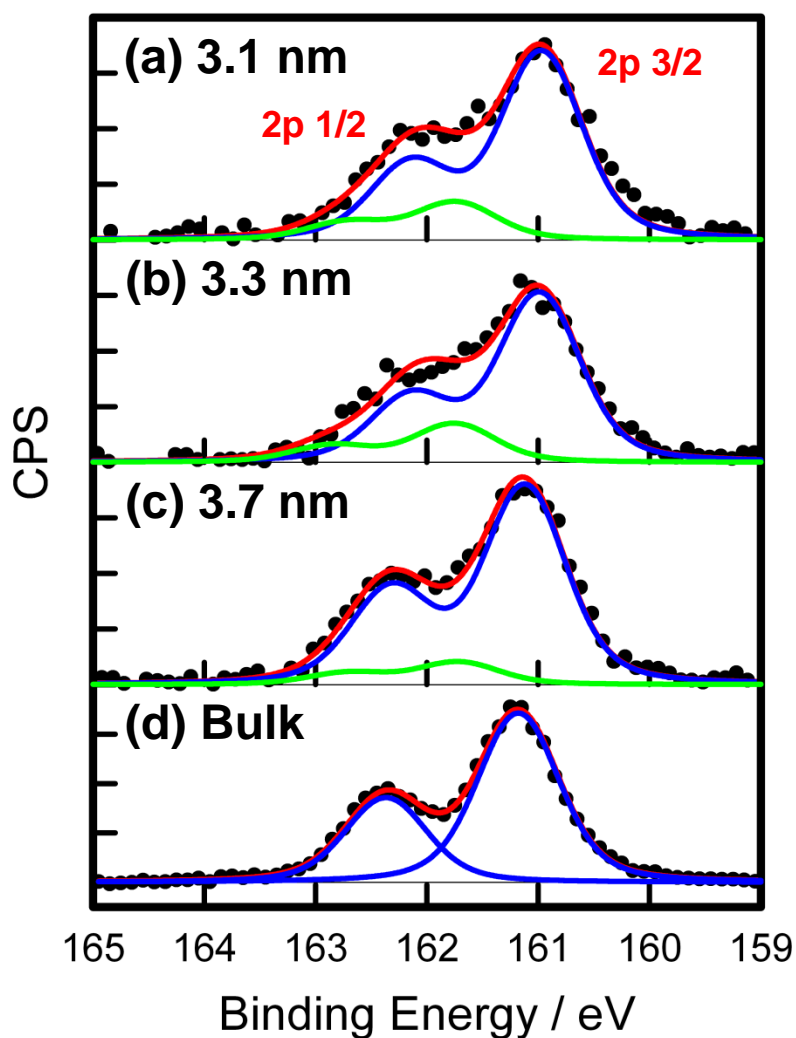
XPS analysis of S 2p regions for CdS QDs

The XPS spectra of S 2p regions for CdS QDs were analyzed using a Voigt function and by comparing those of bulk CdS powder. The fitting results are shown in Fig. S4. The best fit for the bulk CdS spectrum was obtained with a Gaussian band width of 0.70 eV and a Lorentzian band width of 0.29 eV for the spin-orbit split S2p doublet, i.e. S 2p 3/2 region and S 2p 1/2 region. For CdS QDs, the fitting was performed with the same band widths as those from the bulk. Similar to the fitting in the Cd 3d region, at least two sets of spin-orbit split S2p doublet components were required to obtain reasonable fitting. The results are summarized in Table S2. The fits indicate that the signals from core S atoms are dominant, however the peak position shifts lower binding energy with the smaller QD size. The other weaker component appeared in a higher binding energy region. Previous reports explained that, for CdS QDs, the component with a higher binding energy was obtained from the altered chemical environment at the surface, and thus assigned to the S atoms at QD surface.[3, 5] We therefore attribute the observed higher binding energy components to the surface S atoms. The ratio of the surface sulfur to the total sulfur atoms, S_S/S, was calculated from the fitting results and indicated in Table 3. The S_S/S becomes smaller with increase in the QD size, and thus is consistent with the decrease in their surface-to-volume ratio.[5]

Fig. S4. XPS elemental analysis of S 2p regions for CdS QDs with a diameter of (a) 3.1 nm, (b) 3.3 nm and (c) 3.7 nm, and (d) bulk CdS powder. The best fit for bulk CdS XPS peak data was obtained by using a Voigt function with a Gaussian band width of 0.70 eV and a Lorentzian band width of 0.29 eV for both S 2p 3/2 region and S 2p 1/2 region. For CdS QDs, the fitting was performed with the same band width to identify signals from core S atoms (lower binding energy) and from surface S atoms (higher binding energy). Black dots represent raw XPS data, blue lines represent fits for core S atoms, green lines represent fits for surface S atoms, and red lines represent convolution of blue and green lines.

Table S2. XPS peak analysis of the Cd 3d and S 2p regions for CdS QDs and bulk samples. The fitting analysis was conducted using a Voigt function.

QD size / nm	peak	binding energy / eV	Gaussian width / eV	Lorentzian width / eV	FWHM / eV	area
3.1	Cd 3d 5/2	404.63	0.75	0.35	0.95	8278
	Cd 3d 5/2 surface	404.25	0.75	0.35	0.95	3614 (34±6 %)
	Cd 3d 3/2	411.37	0.74	0.34	0.94	6012
	Cd 3d 3/2 surface	410.97	0.74	0.34	0.94	1868 (24±2 %)
3.3	Cd 3d 5/2	404.62	0.75	0.35	0.95	11824
	Cd 3d 5/2 surface	404.27	0.75	0.35	0.95	2143 (15±1 %)
	Cd 3d 3/2	411.39	0.74	0.34	0.94	7982
	Cd 3d 3/2 surface	410.93	0.74	0.34	0.94	1517 (16±3 %)
3.7	Cd 3d 5/2	404.72	0.75	0.35	0.95	16084
	Cd 3d 5/2 surface	404.24	0.75	0.35	0.95	1005 (5.9±1 %)
	Cd 3d 3/2	411.42	0.74	0.34	0.94	11170
	Cd 3d 3/2 surface	410.80	0.74	0.34	0.94	235 (2.1±0.8 %)
Bulk	Cd 3d 5/2	404.65	0.75	0.35	0.95	38313
	Cd 3d 3/2	411.43	0.74	0.34	0.94	26255

QD size / nm	peak	binding energy / eV	Gaussian width / eV	Lorentzian width / eV	FWHM / eV	area
3.1	S 2p 3/2	160.97	0.70	0.29	0.87	711
	S 2p 3/2 surface	161.74	0.70	0.29	0.87	109 (13±4 %)
	S 2p 1/2	162.14	0.70	0.29	0.87	305
	S 2p 1/2 surface	162.71	0.70	0.29	0.87	50 (14±5 %)
3.3	S 2p 3/2	160.99	0.70	0.29	0.87	837
	S 2p 3/2 surface	161.75	0.70	0.29	0.87	122 (13±6 %)
	S 2p 1/2	162.14	0.70	0.29	0.87	345
	S 2p 1/2 surface	162.85	0.70	0.29	0.87	55 (14±6 %)
3.7	S 2p 3/2	161.12	0.70	0.29	0.87	1097
	S 2p 3/2 surface	161.72	0.70	0.29	0.87	85 (7.2±3 %)
	S 2p 1/2	162.32	0.70	0.29	0.87	536
	S 2p 1/2 surface	162.70	0.70	0.29	0.87	44 (7.6±4 %)
Bulk	S 2p 3/2	161.18	0.70	0.29	0.87	3636
	S 2p 1/2	162.37	0.70	0.29	0.87	1820

References

1. J. E. B. Katari, V. L. Colvin and A. P. Alivisatos, *J. Phys. Chem.*, 1994, **98**, 4109-4117.

2. J. Jasieniak and P. Mulvaney, *J. Am. Chem. Soc.*, 2007, **129**, 2841-2848.

3. H. H.-Y. Wei, C. M. Evans, B. D. Swartz, A. J. Neukirch, J. Young, O. V. Prezhdo and T. D. Krauss, *Nano Lett.*, 2012, **12**, 4465-4471.

4. C. J. Powell, A. Jablonski, I. S. Tilinin, S. Tanuma and D. R. Penn, *J. Electron Spectrosc. Relat. Phenom.*, 1999, **98-99**, 1-15.

5. U. Winkler, D. Eich, Z. H. Chen, R. Fink, S. K. Kulkarni and E. Umbach, *Chem. Phys. Lett.*, 1999, **306**, 95-102.